Open Access

Iraqi Journal of Industrial Research (IJOIR)

Journal homepage: http://ijoir.gov.iq

Reducing Corrosion Rate for Electric Water Heater in Welding Joints by Using Sacrificial Anodes

Muthana Mahmood Kassim, Omar Akram Ahmed*, Ahmed Majed Hassan

Iraqi Corrosion Center, Corporation for Research and Industrial Development, Iraq

Article information

Article history:
Received: August, 26, 2025
Accepted: November, 22, 2025
Available online: December, 14, 2025

Keywords:
Electric water heater,
Welding areas,
Sacrificial anode,
Polarization system

Corresponding Author:
Omar Akram Ahmed
omerakramyaseen@yahoo.com

DOI:
https://doi.org/10.53523/ijoirVol12I2ID601

Abstract

Corrosion represents one of the major challenges confronting companies under the Ministry of Industry and Minerals, including the General Company for Electrical Industries, which manufactures electric water heaters typically made of galvanized iron. During the production process, components of the heater are joined using arc welding, where the heat generated during welding causes the removal of the galvanization layer in the welded areas. This results in the development of electrochemical potential differences between galvanized and non-galvanized regions, leading to the formation of localized anodic and cathodic zones. Consequently, electrochemical reactions are initiated, involving the flow of electrons from the anodic to the cathodic regions in the presence of a conductive medium (water), thereby accelerating the corrosion process in the welded zones. In this research, a linear polarization system (Potentiostat MLab-200) was employed to measure the corrosion current density (Icorr) and corrosion potential (Ecorr), followed by the calculation of corrosion rates at various temperatures 30, 40, 50, 60, and 70°C under conditions simulating the actual operation of an electric water heater. The results indicated that the corrosion rate of galvanized iron prior to welding was approximately 2.0 mpy at 70 °C, whereas it increased to 3.0 mpy after welding at the same temperature. To mitigate this corrosion, a sacrificial zinc anode was introduced into the heater system, which reduced the corrosion rate to 1.9 mpy at 70°C. This implementation contributed to prolonging the service life of the heater and enhancing its operational efficiency.

1. Introduction

Corrosion is one of the major challenges affecting carbon steel in various structural components of industrial and oil facilities. Several forms of corrosion may occur, including galvanic corrosion, uniform (general) corrosion, and crevice corrosion. The rate at which corrosion progresses in metals is influenced by multiple factors, such as temperature, exposure duration, the surrounding environmental conditions, and the chemical composition of the metal. Carbon steels are particularly susceptible to corrosion due to their high iron content, which increases their reactivity in corrosive environments [1]. The primary cause of corrosion is the presence of an electrical potential difference-either between the metal and its surrounding environment, between different areas on the same metal surface, or between two dissimilar metals in direct contact. Generally, iron-based structures corrode when they are exposed to a surrounding medium such as soil or water, where electrochemical reactions occur and electron

transfer takes place, resulting in the flow of an electric current. This potential difference may arise due to several contributing factors, including variations in temperature, oxygen concentration, moisture content, or metallurgical differences within the metal itself [2].

1. The properties of a metal may vary across different regions of its structure, or when two dissimilar metals come into contact and exhibit different electrical potentials. This phenomenon commonly occurs in welded areas where metals are joined together.
2. Corrosion may also occur when a new metal is connected to an old one of the same type but with a different potential.

Accordingly, corrosion affects metals as a result of chemical or electrochemical interactions with their surrounding environment. Chemical corrosion arises from the direct reaction between the metal or alloy and the medium in which it is exposed, while electrochemical corrosion occurs due to the flow of electric current through the metal, either from an external potential source or through galvanic coupling between dissimilar metals. Corrosion can manifest in several forms depending on the environmental conditions and the nature of the medium [3], including:

1. Chemical corrosion and electrochemical corrosion.
2. Corrosion caused by high or low temperatures.
3. Dry corrosion and wet corrosion.

The indirect interaction between a metal and corrosive substances leads to electrochemical reactions similar to those occurring in an electrochemical cell when the metal surface comes into contact with an aqueous solution. This phenomenon is referred to as wet corrosion, which represents the primary focus of the present research. Wet corrosion typically occurs when four essential conditions are simultaneously fulfilled: the presence of an electrolyte, an anode, a cathode, and a metallic path that allows electron flow. In the manufacturing of electric water heaters, arc welding is widely used due to several practical advantages: it is cost-effective, offers high operational flexibility, requires minimal space during fabrication, introduces limited thermal distortion, can be applied to various types of metals, and enables welding at different orientations to achieve the desired design. According to a study conducted by M. B. H. Sitorus, the use of electric arc welding showed that the corrosion rate of carbon steel (ST-37) tended to decrease in welded regions when exposed to an $FeCl_3$ solution for an immersion duration of five hours, at a heat input of 0.8108 kJ/mm, reaching a corrosion rate of 68.68 g/m²·h [4]. The working principle of the zinc sacrificial anode is based on its higher electrochemical activity compared to the metal it protects (typically iron or steel). Zinc acts as the anode and gradually corrodes instead of the base metal, thereby transforming the protected surface into a cathodic region that resists oxidation. Consequently, corrosion reactions are effectively inhibited, leading to enhanced durability and an extended service life of the protected structure. Therefore, this research aims to reduce the corrosion rate caused by elevated temperatures in the welded areas of the electric water heater, which occurs due to the removal of the galvanization layer during the welding process. To mitigate this problem, the principle of cathodic protection was applied using a zinc sacrificial anode to provide protection for the metallic surfaces exposed to corrosion in aqueous environments, such as those found in storage tanks and electric water heaters.

2. Experimental Procedure

2.1. Material

Galvanized carbon steel and welded galvanized carbon steel coupons with dimensions of 2 cm × 2 cm were used to evaluate corrosion behaviour in the heat-affected zone (HAZ). In addition, a sacrificial zinc anode coupon (2 cm × 2 cm) was employed for corrosion-rate assessment. For protection evaluation, a 2 cm² sacrificial zinc anode coupon was welded to a galvanized carbon steel coupon to assess its effect on the corrosion rate. A water bath (GFL, Germany) was used to gradually raise the temperature of the test medium to 30, 40, 50, 60, and 70 °C, respectively, to simulate the actual operating conditions of an electric water heater.

2.2. Experimental Setup

the electrochemical measurements were achieved using a potentiostat (MLab 200) with a three-electrode system. The working electrode was galvanized carbon steel. Whereas the counter electrode was Platinum (Pt) with

saturated Ag/AgCl as a reference electrode. The open circuit potential (Ecorr) was monitored for 15 min, as illustrated in Figure (1).

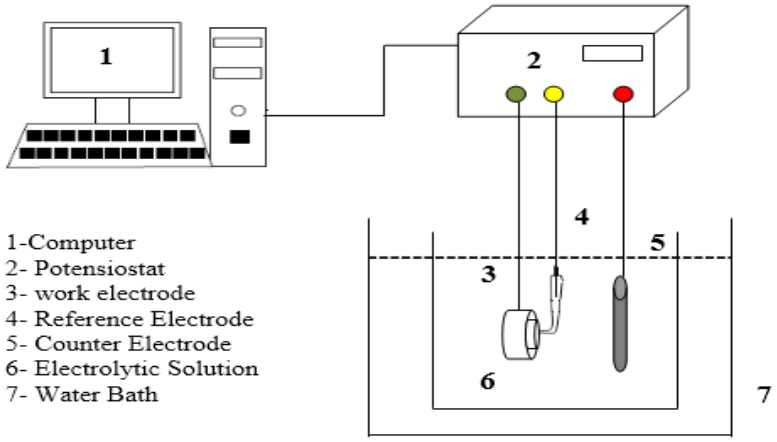

Figure (1): Scheme of the polarization system.

To evaluate the protection of the welded regions, a zinc sacrificial anode coupon was connected to the system, as shown in Figure (2).

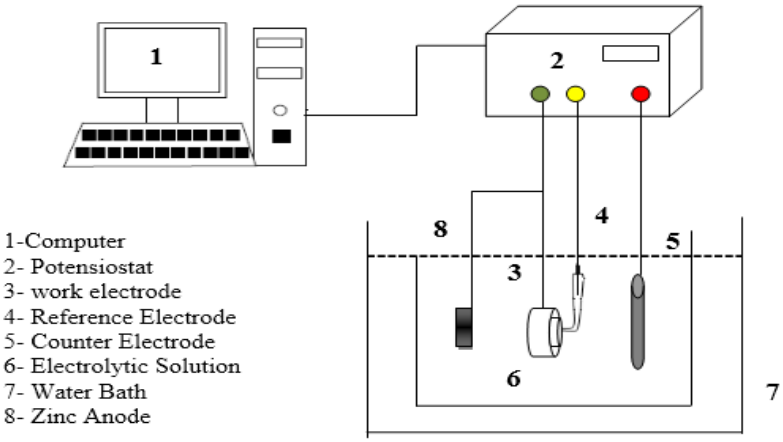

Figure (2): Scheme of the polarization system after the addition of a zinc anode.

2.3. Characterization

The electrical resistance of the water heater was measured using an MC MILLER 400D device. The chemical compositions of the galvanized carbon steel and sacrificial zinc anode coupons were analysed using a Spectro-Metek spectrometer. Surface morphology and elemental composition of galvanized carbon steel coupons were examined using scanning electron microscopy coupled to energy-dispersive X-ray spectroscopy (SEM-EDX, Thermo Fisher Scientific Quattro S).

2.4. Corrosion Rate Calculation

The corrosion rate (C.R) was calculated using Equation (1) [6], considering an exposed surface area of 1 cm^2.

$$\mathbf{C \cdot R = \frac{0.1288 \times Icor \times E{\cdot}W}{\rho}} \quad \text{..... (1)}$$

Where C.R is the corrosion rate measured in units of miles per year (mpy), and 0.1288 is a constant, Icor is the corrosion current density (µA/cm^2), E.W is the equivalent weight of the tested material (g), and ρ is the density (g/cm^3).

3. Results and Discussion

The chemical composition of the galvanized iron used in the heater, as well as that of the zinc anode alloy, was determined using an X-ray fluorescence (XRF) spectrometer. The obtained results are presented in Table (1).

Table (1): Chemical composition of galvanized iron.

Element	Al	Cd	Fe	Pb	Cu	So	Si	P	Ca	Zn
Alloy (wt %)	0.006	0.0003	0.011	0.043	0.0001	0.574	1.018	1.104	0.433	Balance

The chemical composition of the zinc anode alloy was determined and the results of the examination were as in Table (2) and comparing it with the standard (ASTM B-418) [7] regarding the anode showed that it is of the second type, meaning it works in fresh water.

Table (2): Chemical composition of zinc anode.

Element	C	Mn	P	Cr	Si	S	Mo	Ni	Al	Cu	Fe
Alloy (wt %)	0.063	0.16	0.016	0.024	0.025	0.011	0.002	0.015	0.026	0.020	Balance

3.1. Corrosion Mechanism in the Electric Water Heater

Corrosion in an electric water heater occurs when the carbon-steel inner tank is exposed to hot water containing dissolved salts and ions, leading to the formation of an electrochemical cell due to variations in surface electrochemical activity. Defects and weld joints act as anodic sites where iron dissolves into the water, while the less active regions function as cathodic sites that facilitate the reduction of dissolved oxygen or hydrogen ions. These coupled anodic and cathodic reactions produce iron compounds that subsequently transform into iron hydroxides and oxides (rust), causing gradual deterioration of the tank. Table (3) presents the physicochemical characteristics of the medium used to evaluate the corrosion rate.

Table (3): Physical and chemical characteristics of water

Resistance (Ω)	Resistivity (Ω.cm)	Conductivity (µs/cm)	TDS (ppm)
746	746	1340	890

Based on the measured value of total dissolved solids (TDS), expressed in parts per million (ppm) as shown in Table (4), the water was classified accordingly, and the test medium was identified as fresh water.

Table (4): Water classification based on the TDS value.

Classification	Total Dissolved Solids (ppm)
Fresh	<1000
Brackish	1000-10,000
Saline	10,000-100,000
Brine	>100,000

Figure (3) shows the polarization curves obtained for galvanized steel used in the heater, immersed in a fresh-water medium at different temperatures under conditions simulating actual heater operation. The polarization behaiver clearly domestrate that the corrosion rate increaseswith rising temperature. This trend is further supported by the data in Table (5), which show a consistent rise in corrosion intensity as the temperature increases, with the corrosion rate reaching 2.0 mpy at 70 °C. This observation is consistent with the findings of A. S. Alwan *et al*. [8], who investageted the effect of TIG welding on irrigation pipes in southern Iraq . Their results have indicated that the corrosion rate of carbon steel (AISI-1005) in a 3.5% NaCl aquious solution increased to 0.0757 µm/year when the heat input was raised to 5.151 kJ/mm^2. Furthermore, this behavior aligns with previous studies, confirming that the corrosion rate of galvanized iron increases with rising temperature of the surrounding medium [9].

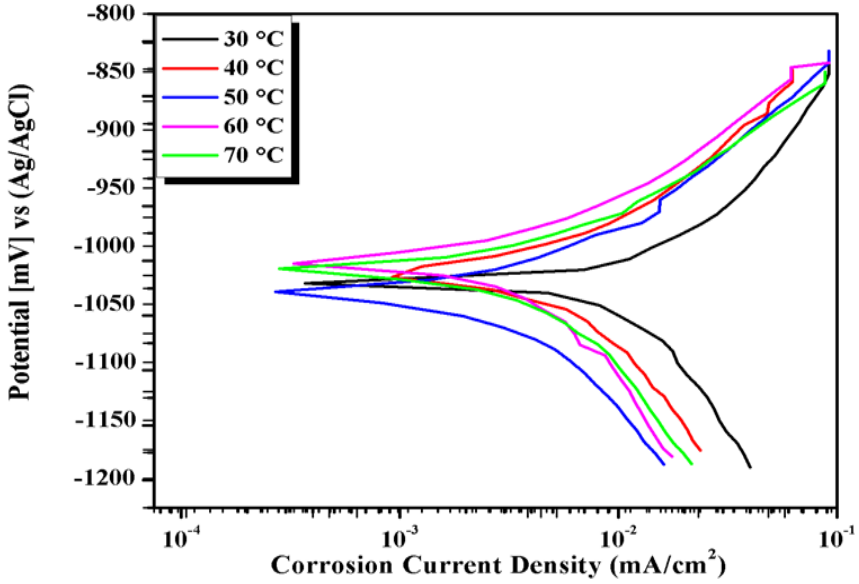

Figure (3): Polarization curves for galvanized iron and for multiple temperatures.

Table (5): Corrosion parameters obtained from polarization curves

Sample	Temperature (°C)	OCP(mV) Time steady state =15 s	Icorr (µA/cm²)	Ecorr (mV)	Corrosion Rate (mpy)
Galvanized Iron	30	-1029	2.24	-1029.5	1.0
	40	-1013	2.97	-1012.2	1.3
	50	-993	3.16	-1017.6	1.4
	60	-988	4.09	-994.4	1.9
	70	-986	4.61	-974.3	2.0

The anodic and cathodic polarization curves presented in Figure (4) for the weld zone of galvanized steel, evaluated in the simulated operating environment of an electric water heater at different temperatures, reveal that the Tafel plots exhibit a clear increase in corrosion rate with rising temperature. This trend confirms the pronounced influence of elevated temperature in accelerating corrosion processes within welded regions. These findings are consistent with the results reported by Hadeel Abdelghani et al. [10], who demonstrated that increasing welding current and welding time leads to higher corrosion rates for carbon steel (SAE 1006) exposed to a 1.0 M H_2SO_4 solution. Furthermore, the results in Table (6) show that the corrosion rate reaches 3 mpy at 70 °C, providing additional evidence that elevated temperatures significantly haste galvanic degradation in the weld zone. This observation aligns with recent studies that similarly report an increase in corrosion rates with rising temperature in the weld zones of galvanized materials [11].

Table (6): Corrosion parameters obtained from polarization curves of the welding area.

Sample	Temperature (°C)	OCP (mV) Time steady state =15s	Icorr (µA/cm²)	Ecorr (mV)	Corrosion Rate (mpy)
Welding	30	-781	3.13	-766.6	1.4
	40	-754	4.08	-738.8	1.9
	50	-748	4.92	-731.6	2.0
	60	-748	6.00	-733.0	2.7
	70	-748	6.55	-760.3	3.0

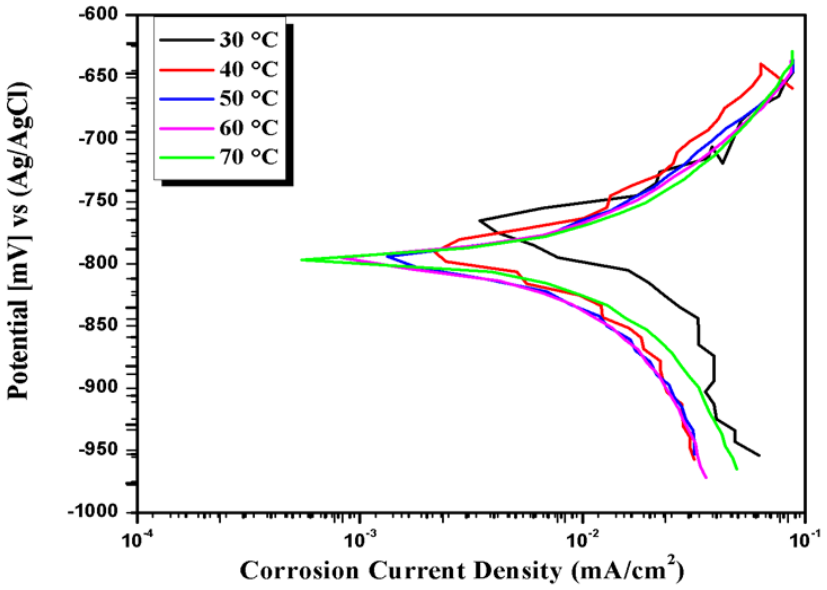

Figure (4): Polarization curves for the welding area and for various temperatures.

Figure (5) presents the anodic and cathodic polarization curves of the sacrificial zinc anode intended for installation within the heater, following its evaluation in freshwater at temperatures different temperature. The polarization data clearly indicate the corrosion current density increases progressively with temperature, resulting in a corresponding rise in the corrosion rate of the zinc anode. This behavior is in agreement with previously reported studies that have highlighted the significant effect of elevated temperatures in accelerating the dissolution of zinc anodes [12]. As shown in Table 7, the corrosion current density of the anode reaches 4.72 µA/cm^2 at 70 °C in the simulated aqueous environment, leading to an estimated anode consumption rate of 2.7 mpy. To maintain effective cathodic protection throughout the operational life of the heater, 10% a safety factor was incorporated into the design, thereby increasing the required anode mass. This design adjustment follows established engineering practices aimed at compensating for the accelerated degradation of sacrificial anodes under elevated-temperature conditions [13].

Table (7): Corrosion parameters obtained from polarization curves of the zinc anode.

Sample	Temperature (°C)	OCP (mV) Time steady state =15s	Icorr (µA/cm^2)	Ecorr (mV)	Corrosion Rate (mpy)
Zinc Anode	30	-1042	1.09	-1062	0.6
	40	-1036	1.71	-1023.3	1.0
	50	-1023	2.7	-115.3	1.6
	60	-1013	3.6	-1004.3	2.0
	70	-1013	4.72	-986.4	2.7

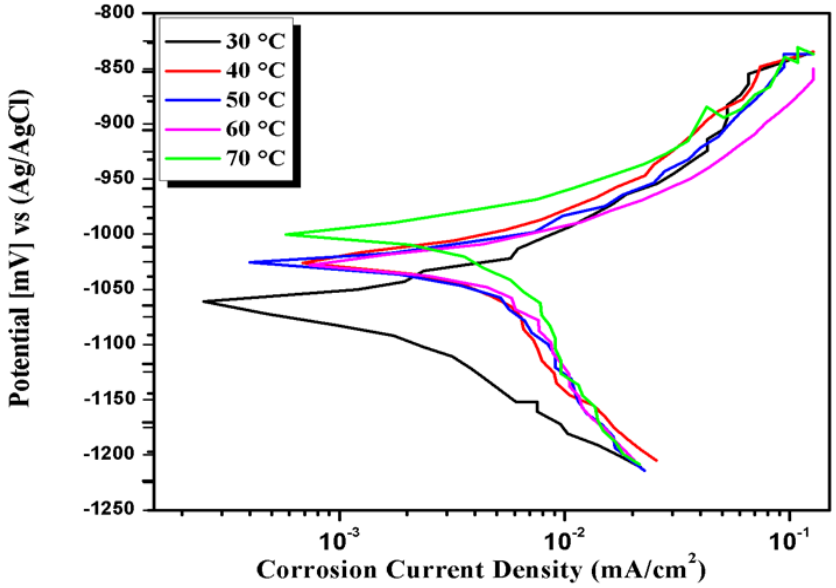

Figure (5): Polarization curves of the zinc anode used at various temperatures.

Figure (6) illustrates the polarization curves of a welded galvanized steel specimen electrically connected to a sacrificial zinc anode and tested in fresh water at different. The polarization behavior clearly shows that coupling the welded galvanized steel to the zinc anode results in a pronounced shift of the corrosion potential toward more negative values, this underscores the role of cathodic protection. This shift reflects the transfer of anodic dissolution to the sacrificial zinc anode, thereby reducing the corrosion current density of the welded galvanized steel compared with its weld zone without protection [14]. As reported in Table 8, the corrosion current density was measured at 4.13 μA/cm², a value comparable to that of the galvanized steel prior to welding (4.61 μA/cm²). Additionally, the corrosion rate of the post-weld galvanized steel decreased from 2.0 mpy to 1.9 mpy following the incorporation of the zinc anode, even at temperatures as high as 70 °C, representative of actual water heater operating conditions. These findings provide clear evidence of the zinc anode's effectiveness in mitigating corrosion within the weld region. This behavior is consistent with previously published works that also report substantial reductions in corrosion rates when sacrificial zinc anodes are employed [15]

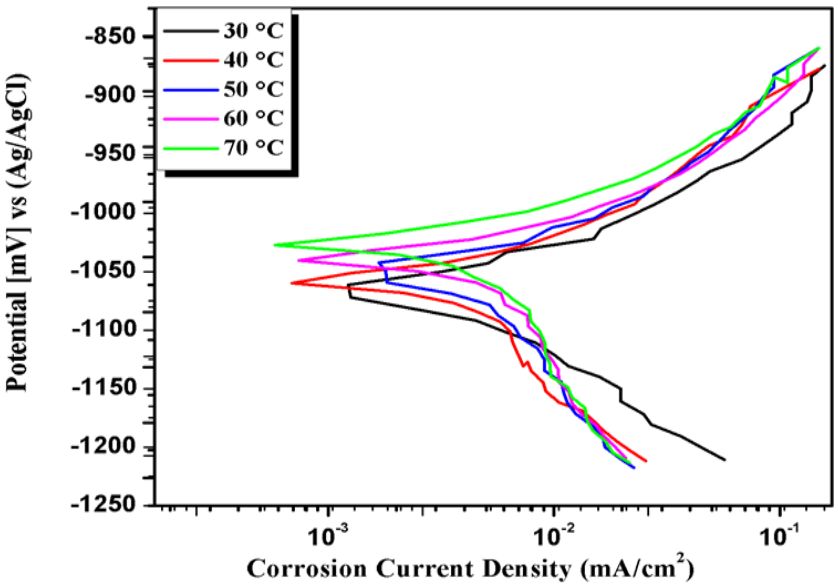

Figure (6): Polarization curves of the weld zone after adding the zinc anode and at various temperatures.

Table (8): Corrosion parameters obtained from polarization curves of the welded area after zinc anode addition.

Sample	Temperature (°C)	OCP (mV) Time steady state =15s	Icorr ($\mu A/cm^2$)	Ecorr (mV)	Corrosion Rate (mpy)
Welding Area + ZINC Anode	30	-1042	1.8	-1071	0.8
	40	-1035	2.36	-1023	1.0
	50	-1022	2.86	-1006.8	1.3
	60	-1017	3.66	-983.3	1.7
	70	-1015	4.13	-977.7	1.9

The surface morphology of the samples was examined before and after welding using Scanning Electron Microscopy (SEM). Figure (7) clearly shows the presence of a uniform zinc coating layer on the surface prior to welding. The surface exhibits a uniform and continuous zinc coating, and the crystalline structure of the protective layer appears well-defined. No cracks or separations are observed, indicating the structural integrity and stability of the zinc layer. The surface texture appears smooth, with no evidence of thermal or mechanical influence. Whereas, Figure (8) demonstrates the complete disappearance of this coating after welding. The high heat input during welding induces noticeable changes in the surface morphology, including the formation of micro-cracks and partial melting or evaporation of the zinc layer, which results in a loss of coating continuity and consequently increases the susceptibility of the underlying metal to corrosion. This confirms that the galvanization layer was removed due to the thermal effect generated during welding. A rough and irregular surface texture was observed, indicating melting and re-solidification of the galvanized layer during the welding process. Numerous studies have investigated the influence of electric arc welding on galvanized steel, including the effect of zinc coating thickness during welding and spot weld strength [15], laser welding on galvanized steel [16], and the effect of gas metal arc welding on galvanized steel [17]. These studies show that residual zinc vapors trapped within the weld zone lead to the formation of porosity, which negatively affects weld strength. SEM and metallographic examinations revealed that zinc residues were detected in porous regions, whereas they were absent in non-porous zones. This confirms that zinc vapor contributes to pore formation during welding [18].

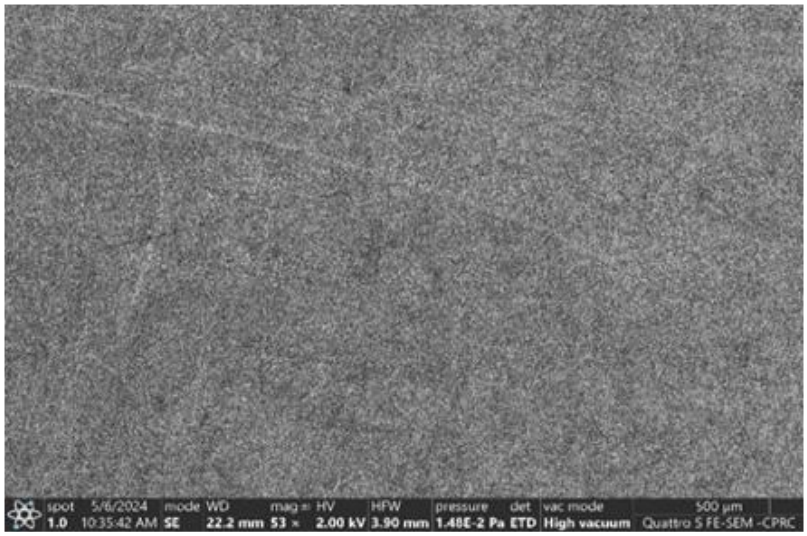

Figure (7): SEM of the sample before Welding.

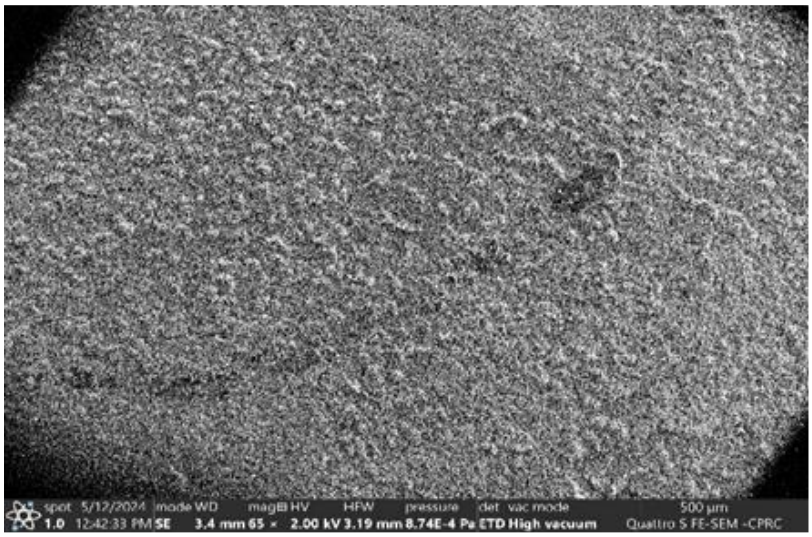

Figure (8): SEM of the sample after welding.

The chemical composition of the welded and non-welded surfaces was analyzed using Energy Dispersive X-Ray Spectroscopy (EDX). Based on the penetration depth of the SEM electron beam, the EDX spectrum of the heater tank metal before welding, shown in Table (9), indicates a predominant zinc content (Zn = 90.3%), confirming the presence of the protective galvanization layer. In contrast, Table (10) shows the EDX spectrum after the welding process, where other metallic elements appear in different proportions due to the welding filler wire used. The zinc percentage dropped sharply to 5.4%, compared to 90.3% before welding, providing direct evidence that the galvanization layer was removed during welding due to the high heat input. Consequently, the exposed steel surface becomes vulnerable to corrosion when subjected to the operating environment of the electric water heater.

Table (9): Chemical compositions before welding.

Element	C	O	Fe	Al	Zn
Weight %	2.9	2.7	2.8	1.4	90.3

Table (10): Chemical compositions after welding.

Element	C	O	Fe	Al	Si	Ca	Mg	Zn
Weight %	3.9	10.3	76.6	2.1	0.5	0.9	0.3	5.4

The surface area of the welding areas in the electric water heater was calculated, on the basis of which the required anode weight was determined. Table (11) shows the area of the area exposed to welding according to the size of the heater.

Table (11): Area exposed to welding.

Capacity (L)	**Exposure area (cm^2)**
120	349.3
180	399.5
220	424.6

The cathodic protection current is determined by knowing the current density and coating efficiency of the structure to be protected, as well as the total surface area of the structure exposed to corrosion. The value of the current density is taken as in Table (12) and the protection current is calculated as in equation (2) [19]

$$I = A \times J \times (1 - CE) \ldots\ldots\ldots (2)$$

Where: I is total protection current (A), A is total surface area of the structure subject to welding in (cm^2), J is required current density (A/cm^2), and CE is coating efficiency (%) (5% coating efficiency was adopted due to the removal of the galvanizing layer as a result of welding).

Table (12): Current density according to the medium [20].

Environment	Current Density (mA/cm^2)
Still fresh water	0.00215 - 0.0043
Moving fresh water	0.0043 - 0.0064
Turbulent fresh water	0.0053 - 0.0161
Hot fresh water	0.0053 - 0.0161
Still seawater	0.0010- 0.0032

The weight of the zinc used to protect the electric heater from corrosion calculated according to equation (3) [21].

$$M = \frac{Icm \times tf \times 8760}{U \times \in} \ldots\ldots\ldots (3)$$

Where M is the anode weight (kg), Icm is the cathodic protection (A), tf is the design life of the system (years), u is the anode utilization factor, ∈: is the theoretical current capacity (A.h/kg), and 8760 represents the number of hours per year.

Table (13): Electrochemical properties of the sacrificial zinc anode.

Electrochemical properties	
Anode Efficiency	90%
Current Capacity (A.hr/kg)	827
Utilization Factor	0.85
Open Circuit Potential(V) vs (Ag/AgCl)	-1.1

A total service life of (15 years) was selected for the water heater, based on the continuous corrosion rate observed in the welded areas. Table (14) presents the weight of the sacrificial zinc anode to be installed inside the heater, depending on its capacity, while Figure (9) shown the geometric configuration of the anode used.

Table (14): Anode weight depending on the capacity of the electric water heater.

Capacity (L)	Anode weight(g)
120	400
180	450
220	500

Figure (9): Sacrificial Zinc Anode.

4. Conclusions

The experimental results demonstrated that welding removed the galvanization layer in electric water heaters, exposing the underlying metal and increasing corrosion rates. The incorporation of a sacrificial zinc anode effectively mitigated corrosion in the welded areas by lowering the corrosion current density. Electrochemical measurements showed a reduction in corrosion rate from 3.0 mpy to 1.9 mpy at 70 °C, with a corresponding shift in corrosion potential to –1015 mV, meeting international cathodic protection standards. Zinc anodes conforming to ASTM B418 Type II proved suitable for freshwater environments, offering a practical, cost-effective means to extend service life beyond 15 years while improving operational efficiency and reducing maintenance costs. Although tested under laboratory conditions, these findings provide guidance for industrial applications, and future studies should consider long-term field evaluations to assess the effects of water flow dynamics and potential biological contamination on the performance of sacrificial-anode cathodic protection systems.

Conflict of Interest: The authors declare that there are no conflicts of interest associated with this research project. We have no financial or personal relationships that could potentially bias our work or influence the interpretation of the results.

References

[1] O. B. S, O. O. T, and A. A, "Effects of Welding Techniques on the Corrosion Resistance of Mild Steel", *South Asian Res. J. Eng. Technol.*, vol. 6, no. 01, pp. 9–19, 2024.

[2] P. Abboud, K. Touma, J. Cherfan, and T. Asmar, "Faculty of Engineering Corrosion of the metals .," no. June, pp. 0–29, 2021.

[3] V. Cicek, "Corrosion Engineering," Corros. Eng., vol. 9781118720, no. October, pp. 1–266, 2014.

[4] Y. Lu, H. Jing, Y. Han, and L. Xu, "Effect of Welding Heat Input on the Corrosion Resistance of Carbon Steel Weld Metal", *J. Mater. Eng. Perform.*, vol. 25, no. 2, pp. 565–576, 2016,

[5] K. A. Natarajan, "Corrosion: Introduction – Definitions and Types", *Ntpel Lect.*, pp. 1–9, 2014.

[6] N. M. Dawood and A. R. K. Abidali, "Influence of titanium additions on the corrosion behavior of Cu-Al-Ni shape memory alloys", *Mater. Sci. Forum*, vol. 1021, pp. 55–67, 2021.

[7] B. ASTM, "B418-12 Standard Specification for Cast and Wrought Galvanic Zinc Anodes," *Annu. B. ASTM Stand.*, vol. 2, no. 4, p. 251, 1988.

[8] H. M. Mohammad, "Effect of Current-Welding on the Corrosion Behavior of Low Carbon Steel (1020) Tig Welding Joints in 3.5% Nacl", *J. Eng. Sustain. Dev.*, vol. 24, no. 4, pp. 1–8, 2020.

[9] A. S. Alwan and S. K. Fayyadh, "Effect of welding heat input on corrosion rate of sprinkler irrigation piping joints by tig welding used in South of Iraq", *Iraqi J. Agric. Sci.*, vol. 50, no. 1, pp. 465–474, 2019.

[10] H. A. Abdulghani, L. Ghalib, and B. J. Nabhan, "Spot Welding Parameters Effect on Surface Corrosion Behavior of Carbon Steel Sheet", *Egypt. J. Chem.*, vol. 65, no. 10, pp. 531–535, 2022.

[11] Y. Lu, H. Jing, Y. Han, L. Xu, "Effect of welding heat input on the corrosion resistance of carbon steel weld metal", *J. Mater. Eng. Perform.*, vol. 25, no. 2 , pp. 565–576, 2016.

[12] M. Zhao *et al.*, "Corrosion Studies of Temperature-Resistant Zinc Alloy Sacrificial Anodes and Casing Pipe at Different Temperatures", *Materials (Basel).*, vol. 16, no. 22, 2023.

[13] K. Gumeni, J. Kola, and J. Minga, "Cathodic protection for cooling water system", *International Scientific Journals.*, vol. 18, no. 1, pp. 25-28, 2024.

[14] L. Guo, F. Xiao, F. Wang, Z. Wei, Y. Zhang, "Effect of post-weld heat treatment temperatures on microstructure, intergranular corrosion resistance, and mechanical properties of 4130 steel with inconel 625 weld overlay", *J. Failure Anal. Prevent.* , vol. 21, no. 5, pp. 1775–1783, 2021.

[15] A. Muazu, Y.S. Aliyu, M. Abdulwahab, A.P.I. Popoola, "Sacrificial anode stability and polarization potential variation in a ternary Al-xZn-xMg alloy in a seawater-marine environment", *J. Marine Sci. Appl.*, vol. 15, no. (2), pp. 208–213, 2016.

[16] S. Shin and S. Rhee, "Porosity characteristics and effect on tensile shear strength of high-strength galvanized steel sheets after the gas metal arc welding process," *Metals (Basel).*, vol. 8, no. 12, 2018.

[17] H. S. Bang, J. C. Kim, B. S. Go, D. W. Choi, and H. S. Kim, "The Pre-Heating Effect for Porosity Control during the Laser Welding of Galvanized Steel Sheets," *Appl. Sci.*, vol. 14, no. 7, 2024.

[18] P. Shreyas, B. Panda, and R. Kumar, "Effect of various welding parameters on the mechanical behaviour of 316l stainless steel-galvanized steel weld," *Mater. Sci. Forum*, vol. 969 MSF, pp. 807–812, 2019.

[19] H. C. Lin, C. A. Hsu, C. S. Lee, T. Y. Kuo, and S. L. Jeng, "Effects of zinc layer thickness on resistance spot welding of galvanized mild steel," *J. Mater. Process. Technol.*, vol. 251, no. March 2017, pp. 205–213, 2018.
[20] A. For, P. Release, and D. Unlimited, "Unified Facilities Criteria (Ufc) Operation and Maintenance : Cathodic Protection Systems," no. November 2016, 2003.
[21] M. N. Jawad, G. Amouzad Mahdiraji, and M. T. Hajibeigy, "Performance improvement of sacrificial anode cathodic protection system for above ground storage tank," *SN Appl. Sci.*, vol. 2, no. 12, pp. 1–8, 2020.
[22] A. G. Ekahasomhi, Y. Ehisuan, and G. Ariavie, "Design of a cathodic protection system for 2,000 barrels crude oil surge tank using zinc anode," *J Multidiscip Eng Sci Technol*, vol. 4, no. 3, pp. 6905–6908, 2017.